Biophysical Chemistry 26 (1987) 357–365
Elsevier

BPC 01151

Three-dimensional representation of chemical gradients

Stefan C. Müller, Theo Plesser and Benno Hess

Max-Planck-Institut für Ernährungsphysiologie, Rheinlanddamm 201, D-4600 Dortmund, F.R.G.

Accepted 27 February 1987

Chemical pattern; Belousov-Zhabotinskii reaction; Oscillating glycolysis; Image evaluation; Two-dimensional spectrophotometry; Perspective graphics

Perspective display techniques are applied to chemical and biochemical data sets. These represent spatially distributed gradients of reactive compounds that participate in pattern-formation processes due to reaction-diffusion or reaction-convection coupling. The patterns form in thin solution layers and are observed as chemical waves in the Belousov-Zhabotinskii reaction, as convection-induced stationary structures during oscillating glycolysis in yeast cytoplasm, and as the diffusive spreading of enzyme-catalyzed metabolic turnover in a substrate layer. The digital data are measured with a two-dimensional spectrophotometer based on a computerized video equipment with high spatial, temporal and intensity resolution. By application of three-dimensional procedures detailed structural properties of chemical and biochemical model systems will be presented yielding localization of reaction and transport events.

1. Introduction

Nature displays a large variety of spatial patterns with a wide range of degrees of complexity, from simple and regular to highly disordered forms. Among the fundamental questions of today are the mechanisms of generation and evolution of such structures and their complex functions. Recently, this area of research has been activated by new methodologies and concepts, originating from various disciplines of science.

One approach to the elucidation of pattern-forming mechanisms is embedded in the concepts and unifying views of nonequilibrium thermodynamics and, more mechanistically, based on the nonlinear dynamics of chemical and biochemical systems in which the coupling of reaction to transport processes such as diffusion or hydrodynamic convection leads to the formation of spatially organized distributions of the reactive compounds. In particular, reaction-diffusion systems with complex kinetic behavior, for instance, the Belousov-Zhabotinskii reaction [1], have proven to be well suited for the study of patterning processes. In biology ample evidence is available for application of this concept to regulatory processes at the subcellular and cellular level, for instance, patterns of aggregating cell colonies [2] or cellular differentiation [3].

In the experimental investigation of global chemical dynamics progress has been achieved in the measurement of spatial patterns, i.e., of stationary or propagating chemical concentration gradients. An instrument which combines precision optics with video and computer technology (a two-dimensional spectrophotometer) allows the determination of chemical concentration distributions in a structured solution layer with high spatial resolution. Suitable software routines have been developed to handle the large amount of information and to extract geometric and kinetic

Dedicated to Professor M. Eigen on the occasion of his 60th birthday.

Correspondence address: S.C. Müller, Max-Planck-Institut für Ernährungsphysiologie, Rheinlanddamm 201, D-4600 Dortmund, F.R.G.

properties from the digital pattern images [4,10].

In this paper we report the application of three-dimensional graphic projections for two-dimensional data fields. The technique is suited for the visualization of structural details and provides new data for the spatial variation of concentration profiles and gradients, thereby retaining all of the quantitative information.

In the following we give a brief description of the instrument and, in some more detail, of the software procedure for three-dimensional graphic representation. The sample preparations are specified and the results for several patterns in the following chemical and biochemical media are presented: (1) excitable solutions of the Belousov-Zhabotinskii (BZ) reaction in which the propagation of circular or spiral-shaped waves of chemical activity is initiated [1,4]; (2) cytoplasm extracted from yeast cells in which the degradation of sugar to alcohol proceeds in an oscillatory manner [5]; or (3) a mixture of reduced nicotinamide adenine dinucleotide (NADH), pyruvate and the enzyme lactate dehydrogenase (LDH) catalyzing the oxidation of NADH.

2. Digital methods

2.1. Two-dimensional spectrophotometry

The instrument for space-resolved digital and computerized spectrophotometric measurements consists of ultraviolet-optical components mounted on a vibration-isolated table for illumination and imaging purposes, a video camera serving as the two-dimensional intensity detector, and a fast, large-memory computer for storage of the digitized data and further data processing.

Important specifications are the spectral sensitivity from 200 to 750 nm of the video camera (Hamamatsu C1000), the image raster resolution of 512×512 picture elements, leading to a spatial resolution down to 4 μm per pixel at the highest magnification, and the intensity resolution of 256 grey levels per pixel. Acquisition and digital storage are feasible at a frequency up to 30 frames per min, limited by the time constant of the camera target and the data transfer from the buffer to the magnetic disk. Thus, the apparatus combines spatial, temporal and intensity resolution in a way which is useful for the analysis of many pattern-formation processes in chemical or biochemical systems. A detailed technical description is given in ref. 4.

2.2. Techniques for two- to three-dimensional transformations

Large two-dimensional arrays are usually represented as variations in luminosity on a black and white or color video monitor [6]. Quantitative information can be visualized by enhancement of specific grey levels which converts the image into a black and white or colored contour map. A more advanced level is reached if color is combined with perspective three-dimensional presentation [7].

The two-dimensional data array of an image recorded by a video camera and stored on the magnetic disk of a computer can be considered as a bivariate function $I = I(x, y)$ with discrete values given at the discrete integer coordinates x and y. Our video camera delivers images with $1 \leq x \leq 512$, $1 \leq y \leq 512$ and $0 \leq I \leq 255$. The two- to three-dimensional transformation allows for looking at the 'object' represented by the data array $I(x, y)$ from different viewpoints as one would inspect a statue by walking around and changing the altitude of the eyes. A three-dimensional image makes the gradients of the function $I(x, y)$ really visible on the two-dimensional display area of a video monitor. A serious problem, especially for a set of rastered data, is the correct removal of hidden lines and surfaces.

In our institute a suitable algorithm has been developed with the following constraints [8]:

(1) orthographic projection;

(2) diffuse illumination so that the intensity of any image element remains unaffected if observed from different viewpoints;

(3) reproduction of the two-dimensional version of the data for zero degree rotation and tilt angle;

(4) linear interpolation of missing points in the three-dimensional projection;

(5) achievement of reasonable processing times and minimization of the propagation of rounding

errors by extensive use of integer arithmetic;

(6) realization of four types of surfaces: dot images with unconnected sample points; profile images with adjacent sample points connected in either the x- or y-direction; cross-hatched or grid images with adjacent sample points connected in both directions; surface images, i.e., cross-hatched images filled by linear interpolation of intensities.

The algorithm is based on a visibility test for each picture element drawn. The test is performed by a slightly modified Bresenham line algorithm [9].

The FORTRAN 77 code of the algorithm was integrated into the GRIPS package [4] for interactive raster graphics. This software package runs on a Perkin-Elmer computer and supports the graphics workstation Raster Technology model ONE/80 (8-bit depth) equipped with a high-resolution monitor (1280 × 1024 pixels).

In section 4 the procedure of rendering two-dimensional images in three-dimensional perspective is applied to a representative selection of chemical patterns. The images show gradients in transmitted light intensity which are similar to the corresponding concentration gradients and reveal all the noteworthy features rendered by the three-dimensional display techniques. For an evaluation of the collected data in terms of spatial concentration distributions the recorded intensity patterns have to be transformed into absorbance values by using a spatio-temporal (two-dimensional) version of Lambert-Beer's law [4]. The pixel noise in all images has been reduced by a 3 × 3 pixel moving average.

3. Materials

Reagent-grade chemicals were used throughout. All solutions were filtered using 0.44 μm Millipore filters. The ambient temperature was 24 ± 1°C. A variety of solutions showing spatial pattern formation were investigated: (1) A quiescent but excitable Belousov-Zhabotinskii system was obtained by preparing a solution of 48 mM NaBr, 342 mM $NaBrO_3$, 95 mM $CH_2(COOH)_2$, 376 mM H_2SO_4. Ferroin (3.5 mM) was added about 2 min later. A volume of the mixture resulting in a 1-mm layer was placed in a siliconized dust-free petri dish of 6.8 cm diameter. A circular wave was initiated by releasing a small amount of a solution containing 0.48 M $NaBrO_3$ and 0.5 M H_2SO_4 from a micropipet. The procedure for triggering a spiral wave is described in ref. 10. Observations were carried out at 490 nm (maximum ferroin absorption). The petri dish was covered with a glass plate. For the observation of convective effects on chemical waves, slightly different reaction mixtures were used in layers of increased thickness (up to 1.8 mm) and the glass cover was removed. (2) A cytoplasmic medium was extracted from commercial baker's yeast cells (*Saccharomyces cerevisiae*) according to a published procedure [11]. The protein content was about 50 mg/ml. The extract was supplied with glycogen and potassium phosphate buffer, leading to oscillations of metabolic activity. Periodically reappearing patterns were observed by monitoring the absorption of NADH at 370 nm in a layer of 1.8 mm thickness placed in a dish of 3.2 cm diameter. (3) A 5 μl drop of enzyme solution (LDH suspended in 50% glycerol and 80-fold diluted with 0.1 M triethanolamine hydrochloride (TRA) buffer) was placed by a micromanipulator on the surface of a solution layer of 1.8 mm thickness containing 2.4 mM NADH and 2.8 mM pyruvate in 0.1 M TRA buffer. The oxidation of NADH catalyzed by LDH was recorded at 370 nm.

4. Results

In fig. 1 the perspective technique is applied to a simple pattern, a half-section of a circular chemical wave in an excitable layer of the BZ reaction. The grid image illustrates the pronounced difference between the steepness of the outer wave front that propagates radially into the surrounding quiescent medium and the much smoother slope of the relaxing back of the wave which leads to the formation of a broad trough. The gradient of ferroin concentration of the excited front reaches 17 mM/mm while it does not exceed 3 mM/mm on the back of the wave.

A more complex pattern can be produced in the BZ reaction by disruption of the front of a target pattern of circular geometry resulting in

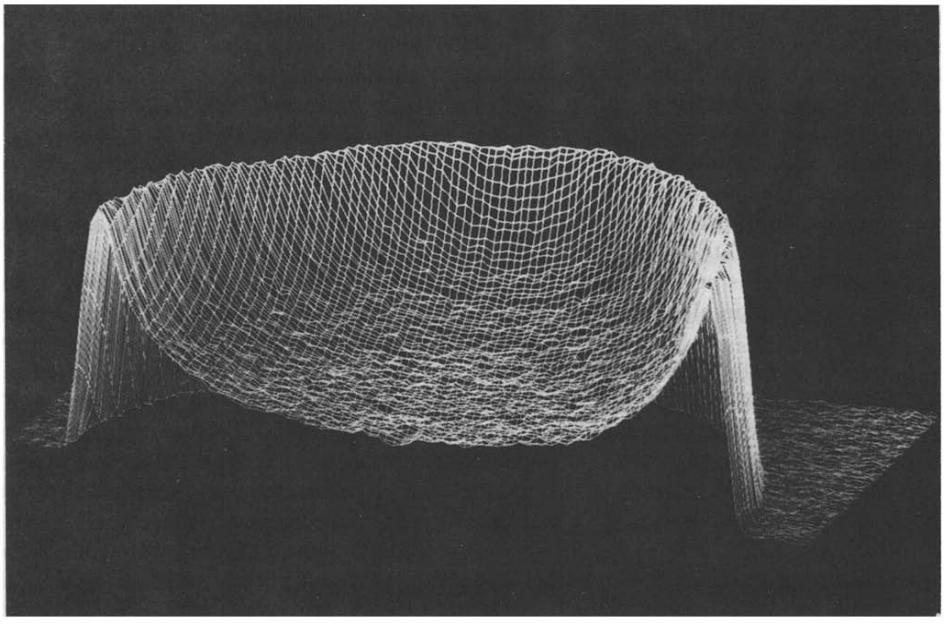

Fig. 1. Circular wave of chemical activity in a 1 mm layer of an excitable BZ reaction, presented as a grid image in three-dimensional perspective, rotated clockwise by 20° and tilted by 70°. The image shows the measured grey levels of transmitted light intensity (490 nm) of 450×210 pixels corresponding to approx. one-half (9×4 mm^2) of a two-dimensional image published in fig. 2 of ref. 4.

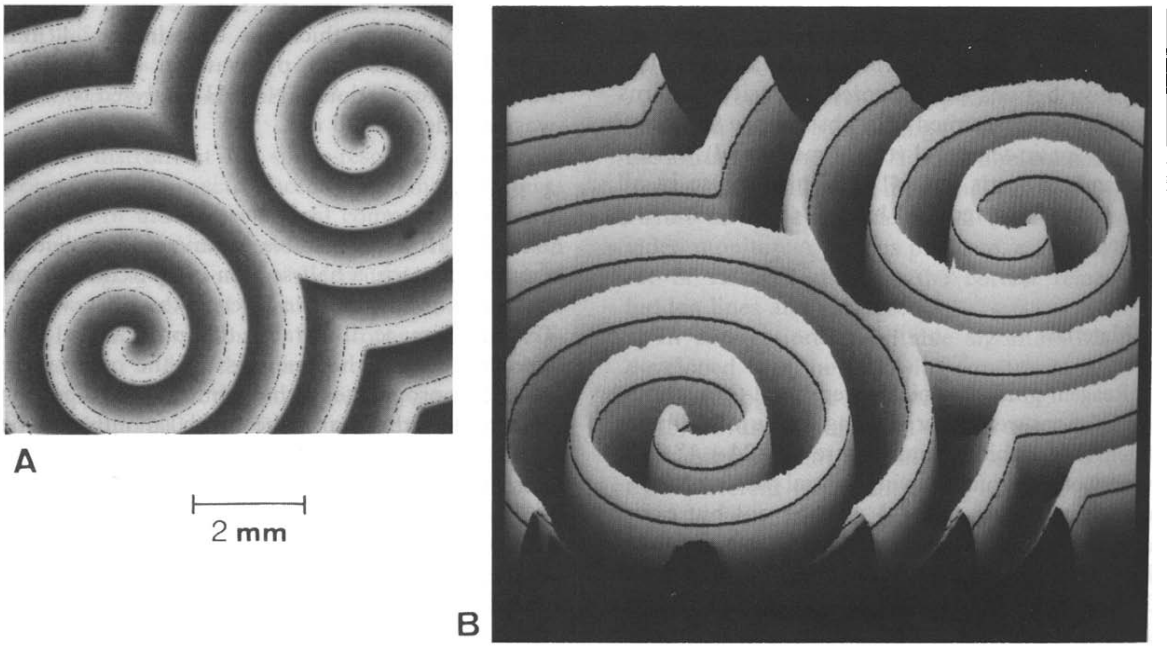

Fig. 2. Symmetric pair of spiral waves in a 1 mm layer of an excitable BZ reaction. The grey levels of transmitted light intensity (490 nm) measured for the 410×410 pixels in panel A are connected by linear interpolation (surface image) and displayed in panel B in three-dimensional perspective at a tilt angle of 45°. The narrow grey level interval enhanced in black is the same in both images.

spiral-shaped rotating waves [10]. The snapshot in fig. 2A shows a pair of such waves with inward-turning tips, i.e., with the opposite sense of rotation. A surface image is used for rendering the shape of the intensity gradients in three-dimensional perspective (fig. 2B). In contrast to the two-dimensional display, this presentation allows one to recognize in detail the height of the wave crest and its modulation at the collision area between both fronts where the two waves start to annihilate each other. In terms of chemistry the dip at the area of interaction indicates a more reduced state of the catalyst and indicator ferroin produced by the collision. The crest, which marks the spatial transition between oxidation and reduction of the catalyst, reveals local chemical features of the oscillatory reaction kinetics to be analyzed further.

The intensity level enhanced in black shows that the transformation to three-dimensional perspective retains the isoconcentration lines. It emphasizes the geometric regularity of the pattern which is found to be well described by Archimedian spirals except for the core region close to the spiral tip, where no wave propagation has been observed [10]. One of the particular features is demonstrated in fig. 3. An image of the tip taken at much higher spatial resolution is transformed into a three-dimensional profile image showing that the shape of the wave profile is more symmetric close to its tip than at locations outside the spiral core, for instance, at the front edge of the three-dimensional picture. The gradients of ferroin concentration at the steep slopes reach 5 mM/mm, those at the smoother slopes are less than 1 mM/mm. These values are about 3-times smaller than those of the corresponding gradients in the circular wave shown in fig. 1.

Additional structuralization processes in the BZ reaction can be displayed by allowing convective currents to evolve in the solution layer. Whereas the previous experiments were carried out under

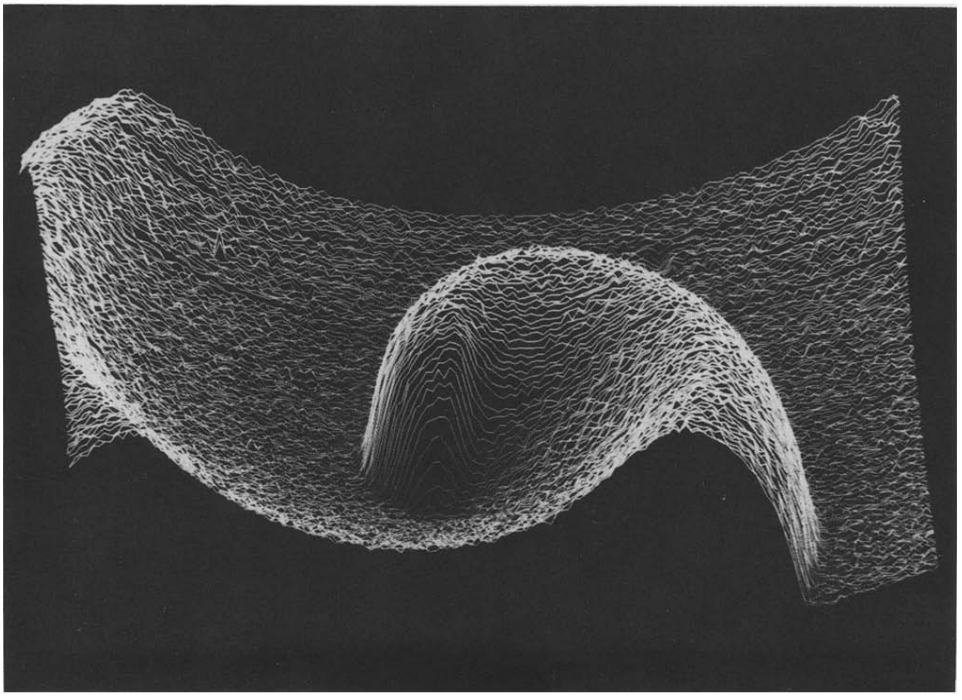

Fig. 3. Frontal view of the tip of the spiral wave in the BZ reaction. The three-dimensional profile image with a tilt angle of 55° is derived from a 450×310 pixel section of a spiral image and corresponds to an area of 2×1.4 mm^2.

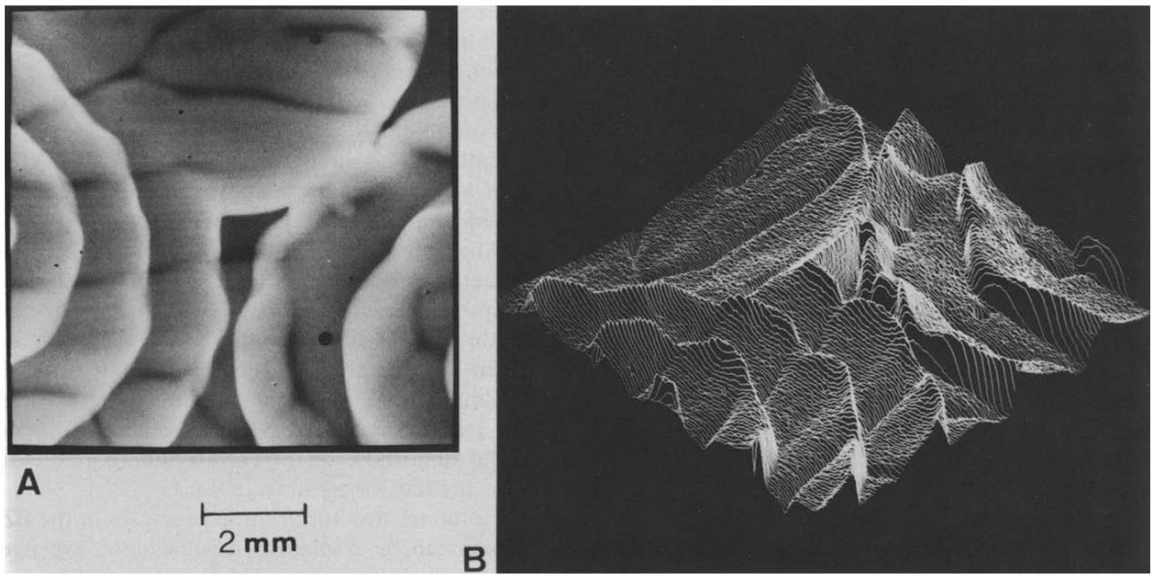

Fig. 4. Propagation of chemical wave fronts in an open convecting solution layer of the BZ reaction (depth 1.4 mm). The transmitted light intensity of the 450×450 pixels in panel A, showing both wave fronts and boundaries of convection rolls, is represented in panel B as a three-dimensional profile image, rotated anticlockwise by 45° and tilted by 45°.

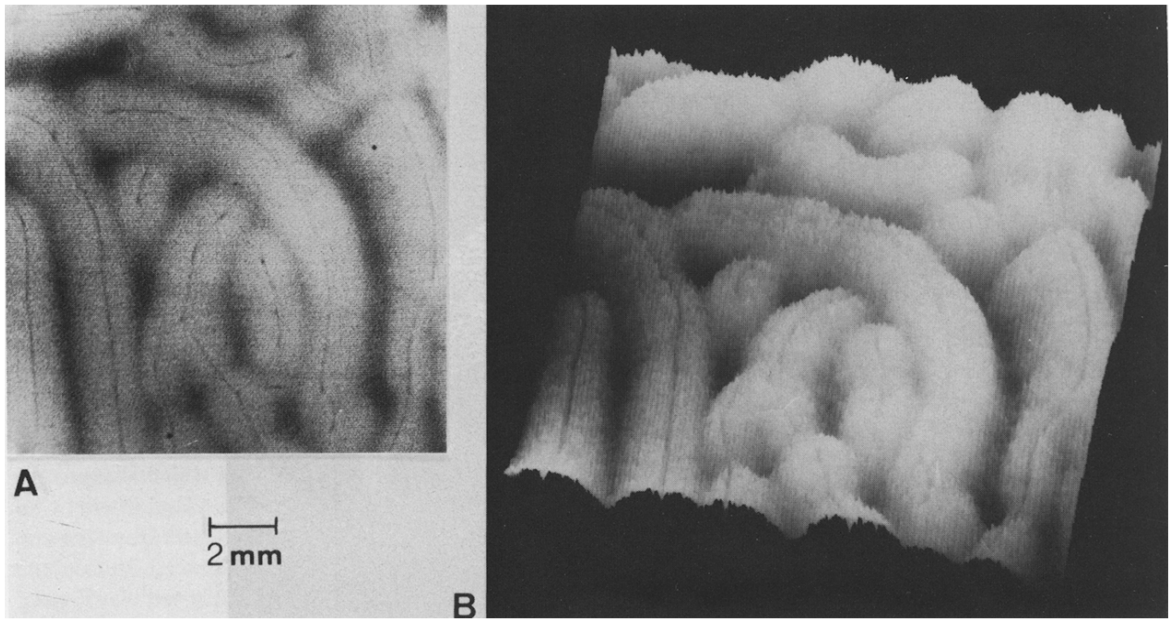

Fig. 5. Spatial pattern of NADH in an open 1.8 mm layer of cytoplasm extracted from yeast cells, as observed by light absorption at 370 nm during oscillating glycolysis. The 420×450 pixel image A is represented in panel B as a slightly rotated three-dimensional surface image at a tilt angle of 45°.

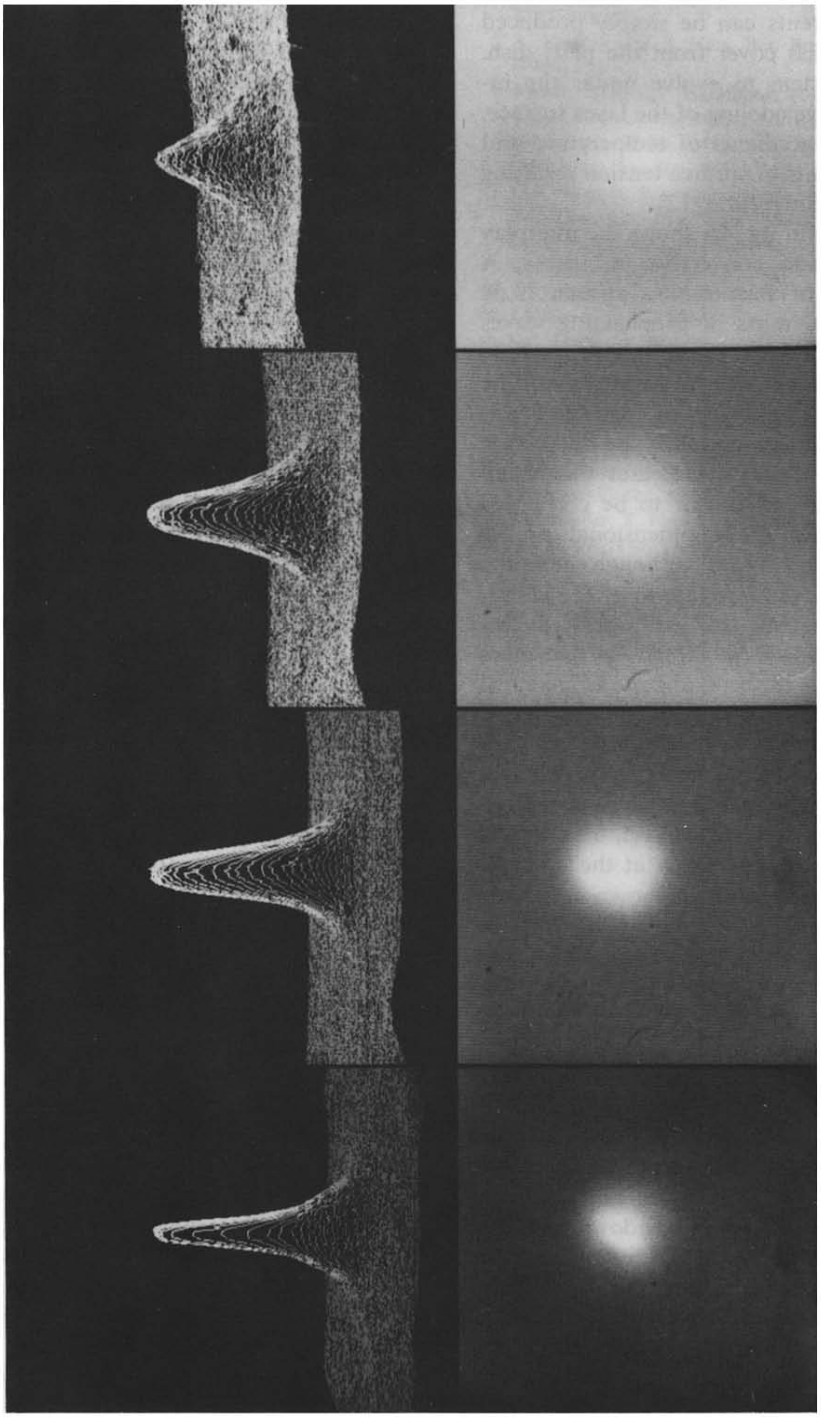

Fig. 6. Diffusion in a 1.8 mm layer of pyruvate/NADH solution after addition of a drop of the enzyme LDH, which catalyzes the biochemical turnover. The four lower images of light intensity transmitted at 370 nm show a time sequence taken 3, 8, 18 and 32 min after addition of LDH (from left to right). They are scaled versions of the original 450×450 pixel images. The upper row shows the corresponding three-dimensional profile images at a tilt angle of 75°.

isothermal conditions (less than $\pm 0.1°C$ across the layer) such currents can be simply produced by removing the glass cover from the petri dish. This allows the system to evolve under the influence of evaporative cooling of the layer surface, which gives rise to gradients of temperature and consequently gradients of surface tension resulting in Marangoni-type convection [12].

The digital image in fig. 4A shows the interplay between diffusive and convective influences. A low concentration of ferroin was chosen (0.64 mM) for which the fronts of propagating waves and a stationary network of dark lines can be simultaneously detected. The latter might well be an indication of the boundaries of convective currents [12,13], a problem currently being further analyzed. Panel A of fig. 4 indicates that small distortions of the fronts appear to be correlated with these lines. The three-dimensional profile graph in panel B of fig. 4, although its quite peculiar form makes the recognition of the identical structure somewhat difficult, nevertheless renders this correlation more directly in that there are pronounced clefts in the landscape of chemical wave crests.

Different patterns are observed in thin layers of yeast extract at wavelengths specific for NADH absorption. They form repetitively during oscillating glycolysis, as first reported in ref. 5. A digital image of a rod-like pattern taken at the moment of maximum intensity contrast is shown in fig. 5A. Such a pattern typically occurs during the first one or two oscillation periods. It has been shown that the pattern morphology is mainly determined by a network of convection rolls or Bénard-type cells [13], probably analogous to the effects described above for the BZ reaction.

The three-dimensional surface image in panel B of fig. 5 displays the smooth variation of the NADH concentration in the immediate neighborhood of the thin dark lines in the center of the bright areas. These lines are shadows cast by pronounced gradients of refractive index close to the boundaries of convective currents and reflect the spatial arrangement of the convective pattern. The three-dimensional version of the NADH pattern certainly has some similarity with hydrodynamic flow patterns in the real three-dimensional world.

A locally initiated transport process in an enzymatic reaction is demonstrated in the sequence of panels in fig. 6. A small drop of the enzyme LDH is pipeted into a solution layer containing the substrates NADH and pyruvate at almost equal concentrations. The surface tension of the drop is adjusted to that of the layer minimizing disturbances at the moment of drop addition. The two-dimensional images (lower row in fig. 6) are obtained by NADH absorption and show how the initially small, bright center of enzyme activity becomes larger in time while converting NADH to NAD and pyruvate to lactate. The upper row of fig. 6 presents the same data sets as three-dimensional profile images. The shape of the profiles roughly corresponds to that expected from the solution of appropriate reaction-diffusion equations. Thus, one can assume that the spreading is governed by diffusion processes (cf. different experimental conditions in ref. 4). In the temporal sequence of the perspective images the point of maximum brightness (minimum NADH concentration) remains constant in height, while the background gradually moves upward. The decrease of the amplitude is accompanied by an increase of the half-width of the bell-shaped curves. In this system fast diffusion of NADH/NAD and pyruvate/lactate is coupled with slow diffusion of the enzyme molecules. Evaluation of the individual diffusion constants requires further experimental and theoretical efforts.

5. Concluding remarks

There is an increasing number of scientific areas in which the phenomenological or quantitative characterization of pattern-forming systems has been recently improved. One important reason for this development is the rapidly increasing efficiency with which video cameras linked to computer systems can be used in the laboratory. This type of digital technique is readily applied to biological research. Examples are the analysis of fluorescence patterns on a cellular scale [14,15] or improvement of the resolution in classical light microscopy [16]. Quantitative results measured in chemical and biochemical systems have begun to appear in the literature [10,17].

In this paper we demonstrate that a three-dimensional perspective display of two-dimensional digital data sets enhances the perception of local details of chemical patterns, for instance, the identification of areas of wave collision and spatial cores. Such details reveal important properties of the mechanisms of pattern formation. The graphic technique is helpful in rendering particular aspects of forms that may otherwise not be recognized. The advantage over other techniques, e.g., contrast enhancement, contour maps, or pseudo-colors, becomes obvious with increasing structural complexity [18]. So far the method has given highly interesting results on a mostly qualitative basis. Since none of the information in an image is lost, further quantification of the chemical gradients and their distribution in two-dimensional space can be obtained and is currently being carried out.

References

1 A.N. Zaikin and A.M. Zhabotinskii, Nature 225 (1970) 535; R.J. Field and M. Burger, Oscillations and traveling waves in chemical systems (Wiley, New York, 1985).
2 G. Gerisch, Naturwissenschaften 58 (1971) 430.
3 H. Meinhardt, Models of biological pattern formation (Academic Press, London, 1982).
4 S.C. Müller, T. Plesser and B. Hess, Naturwissenschaften 73 (1986) 165.
5 A. Boiteux and B. Hess, Ber. Bunsenges. Phys. Chem. 84 (1980) 392.
6 Raster Graphics Handbook (Conrac Division, Conrac Corp., Covina, CA, 1980); P.J. Bouma, Physical aspects of colour, eds. W. de Groot, A.A. Kruithof and J.L. Develtjes (McMillan, London, 1971).
7 D.F. Rogers, Procedural elements for computer graphics (McGraw-Hill, New York, 1985). J.D. Foley and A. van Dam, Fundamentals of interactive graphics (Addison-Wesley, London, 1983).
8 W. Kramarczyk, (1987) NATO ASI Series F.
9 J.E. Bresenham, IBM System J. 4 (1965) 25.
10 S.C. Müller, T. Plesser and B. Hess, Science 230 (1985) 661; S.C. Müller, T. Plesser and B. Hess, Physica 24D (1987) 71, 87.
11 B. Hess and A. Boiteux, Hoppe-Seyler's Z. Physiol. Chem. 349 (1968) 1567.
12 J.K. Platten and J.C. Legros, Convection in liquids (Springer-Verlag, Berlin, 1984).
13 S.C. Müller, T. Plesser, A. Boiteux and B. Hess, Z. Naturforsch. 40c (1985) 588.
14 R.Y. Tsien and M. Poenie, Trends Biochem. Sci. 11 (1986) 450.
15 N. Stockbridge and W.N. Ross, Nature 309 (1984) 266.
16 R.D. Allen, Annu. Rev. Biophys. Biophys. Chem. 14 (1985) 265.
17 C. Vidal, A. Pagola, J.M. Bodet, P. Hanusse and E. Bastardie, J. Phys. 47 (1986) 97.
18 A.F. Hasler, H. Perce, K.R. Morris and J. Dodge, Bull. Am. Meteorol. Soc. 66 (1985) 795.